JrnlID 12035_ArtID 956_Proof# 1 - 09/02/2018

Molecular Neurobiology
https://doi.org/10.1007/s12035-018-0956-5

Increased Levels of Rictor Prevent Mutant Huntingtin-Induced Neuronal Degeneration

Jordi Creus-Muncunill[1,2,3] · Laura Rué[1,2,3,4] · Rafael Alcalá-Vida[1,2,3] · Raquel Badillos-Rodríguez[1,2,3] · Joan Romaní-Aumedes[1] · Sonia Marco[5] · Jordi Alberch[1,2,3] · Isabel Perez-Otaño[5] · Cristina Malagelada[1] · Esther Pérez-Navarro[1,2,3]

Received: 31 October 2017 / Accepted: 6 February 2018

Abstract

Rictor associates with mTOR to form the mTORC2 complex, which activity regulates neuronal function and survival. Neurodegenerative diseases are characterized by the presence of neuronal dysfunction and cell death in specific brain regions such as for example Huntington's disease (HD), which is characterized by the loss of striatal projection neurons leading to motor dysfunction. Although HD is caused by the expression of mutant huntingtin, cell death occurs gradually suggesting that neurons have the capability to activate compensatory mechanisms to deal with neuronal dysfunction and later cell death. Here, we analyzed whether mTORC2 activity could be altered by the presence of mutant huntingtin. We observed that Rictor levels are specifically increased in the striatum of HD mouse models and in the putamen of HD patients. Rictor-mTOR interaction and the phosphorylation levels of Akt, one of the targets of the mTORC2 complex, were increased in the striatum of the R6/1 mouse model of HD suggesting increased mTORC2 signaling. Interestingly, acute downregulation of Rictor in striatal cells in vitro reduced mTORC2 activity, as shown by reduced levels of phospho-Akt, and increased mutant huntingtin-induced cell death. Accordingly, overexpression of Rictor increased mTORC2 activity counteracting cell death. Furthermore, normalization of endogenous Rictor levels in the striatum of R6/1 mouse worsened motor symptoms suggesting an induction of neuronal dysfunction. In conclusion, our results suggest that increased Rictor striatal levels could counteract neuronal dysfunction induced by mutant huntingtin.

Keywords Akt · mTOR · Raptor · S6K · Striatum

Jordi Creus-Muncunill and Laura Rué contributed equally to this work.

Electronic supplementary material The online version of this article (https://doi.org/10.1007/s12035-018-0956-5) contains supplementary material, which is available to authorized users.

✉ Esther Pérez-Navarro
estherperez@ub.edu

[1] Departament de Biomedicina, Facultat de Medicina i Ciències de la Salut, Institut de Neurociències, Universitat de Barcelona, Casanova 143, E-08036 Barcelona, Catalonia, Spain

[2] Institut d'Investigacions Biomèdiques August Pi i Sunyer (IDIBAPS), Barcelona, Catalonia, Spain

[3] Centro de Investigación Biomédica en Red sobre Enfermedades Neurodegenerativas (CIBERNED), Cáceres, Spain

[4] Present address: Department of Neurosciences, Experimental Neurology; VIB Center for Brain & Disease Research, Laboratory of Neurobiology, KU Leuven – University of Leuven, Leuven, Belgium

[5] Laboratorio de Neurobiología Celular, Centro de Investigación Médica Aplicada y Universidad de Navarra, Pamplona, Spain

Introduction

Mechanistic target of rapamycin (mTOR) is a serine/threonine kinase that controls multiple cellular functions [1]. To exert its kinase activity, mTOR binds to specific accessory proteins to form two distinct multi-protein complexes, the mTOR complex 1 (mTORC1) and 2 (mTORC2). One of the important and exclusive components of mTORC1 is Raptor (regulatory-associated protein of mTOR), while Rictor (rapamycin-insensitive companion of mTOR) characterizes mTORC2 [2–4]. Each complex phosphorylates specific substrates to regulate different cell processes. Thus, mTORC1 regulates mRNA translation through the phosphorylation of eukaryotic translation initiation factor 4E-binding protein 1 and p70S6 kinase (S6K) [5], and autophagy by phosphorylation of unk-51 like autophagy activating kinase 1 (Ulk1; [6]. Although the function of mTORC2 is not as well defined, it has been shown that it phosphorylates Akt [7], serum- and glucocorticoid-induced protein kinase (SGK) [8] and protein kinase C [4,

9], thereby regulating different processes such as cell survival and reorganization of actin cytoskeleton [10].

mTOR signaling regulates important neuronal functions and consequently, alterations in the activity of both mTORC1 and 2 have been reported in neurodevelopmental, neurodegenerative, and psychiatric disorders (for review, see [11, 12]. Increased mTORC1 activity occurs for example in Alzheimer's disease [13] and in fragile X syndrome [14], whereas decreased mTORC2 activity, due to Rictor deletion, has been linked to schizophrenia [15] and affects the size and function of cerebellar neurons [16]. In Huntington's disease (HD), only mTORC1 activity has been analyzed and conflicting results have been reported [17–19]. This disease is caused by an abnormal expansion of a CAG repeat in the exon-1 of the huntingtin (*htt*) gene [20] that generates a mutant htt (mhtt) protein. Although htt expression is ubiquitous, the most remarkable neuropathological feature of HD brain is the progressive loss of medium-sized spiny neurons occurring in the striatum (caudate and putamen), which is classified from Vonsattel grade 0–4 [21].

Mhtt is involved in a large amount of toxic effects that trigger cell dysfunction (reviewed in [22, 23]. Although, mhtt is expressed since birth HD symptoms appear during adulthood. Thus, it is plausible that several mechanisms may be activated to deal with neuronal dysfunction and later cell death, which may be responsible for the gradual nature of HD progression. The majority of the mouse models developed so far is characterized by the presence of motor and cognitive dysfunction without, or with mild, striatal cell loss [24]. Activation of compensatory mechanisms has been shown in cells expressing mhtt which could account for the absence or low cell death in the striatum of HD mouse models (for review, see [25]). One of the pro-survival mechanisms activated in the striatum of these animals, and in cellular models of HD, is the PI3K/Akt pathway [26, 27]. We have shown that decreased levels of the PH domain leucine-rich repeat protein phosphatase 1 contribute to maintain high levels of phospho (p) Ser473 Akt in striatal cells expressing mhtt [27]. Although we observed decreased levels of PHLPP1 in the striatum, cortex and hippocampus of R6/1 mouse model of HD, increased pSer473 Akt levels were detected only in the striatum suggesting that other mechanisms should be involved in Akt overactivation in this brain region. Here, we hypothesized that mTORC2 activity could be enhanced in the striatum of HD contributing to increase the phosphorylation of Akt at Ser473. According to our hypothesis, we show that mTORC2 activity is increased in the striatum of HD likely due to increased Rictor levels. Interestingly, acute downregulation of Rictor in cells expressing mhtt increased, whereas acute upregulation prevented, cell death in vitro. In addition, downregulation of Rictor in the striatum of a mouse model of HD worsened motor learning and coordination, and induced cell death. Thus, our results show that mTORC2 activity is altered in HD striatum suggesting that increased activity of this pathway could temporarily prevent neuronal death.

Materials and Methods

HD Mouse Models

Genotyping and CAG repeat length determination of male R6/1 and R6/2 heterozygous transgenic mice (B6CBA background) expressing the exon-1 of mhtt with 145 and 90 CAG repeats, respectively, were performed as previously described [28]. Our R6/1 mice colony expresses 145 CAG repeats instead of 115 CAG repeats of the original R6/1 mice, while R6/2 mice express 90 CAG repeats instead of 150 CAG repeats of the original R6/2 mice due to CAG repeat instability as has been previously described by other groups [29–31]. Homozygous mutant $Hdh^{Q111/Q111}$, with targeted insertion of 109 CAG repeats that extends the glutamine segment in murine huntingtin to 111 residues and wild-type $Hdh^{Q7/Q7}$knock-in mice, were obtained from heterozygous $Hdh^{Q111/Q7}$ breeding pairs as described previously. YAC128 mice (line 55 homozygotes) in FVB/N background contain full-length human *HTT* with 128 CAG repeats [32]. Only males were used for all experiments. All mice were housed together in numerical birth order in groups of mixed genotypes, and data were recorded for analysis by microchip mouse number. Experiments were conducted in a blind-coded manner respect to genotype. Animals were housed with access to food and water ad libitum in a colony room kept at 19–22 °C and 40–60% humidity, under a 12:12-h light/dark cycle. All procedures were performed in compliance with the NIH Guide for the Care and Use of Laboratory Animals and approved by the local animal care committee of Universitat de Barcelona following European (2010/63/UE) and Spanish (RD53/2013) regulations for the care and use of laboratory animals.

Post-mortem Human Brain Tissue

Samples from HD patients and control individuals (putamen and frontal cortex) were obtained from the Neurological Tissue Bank of the Biobank-Hospital Clínic-Institut d'Investigacions Biomèdiques August Pi i Sunyer (IDIBAPS; Barcelona, Catalonia). Details are provided in supplementary Table S1. Human samples were obtained following the guidelines and approval of the local ethics committee (Hospital Clínic of Barcelona's Clinical Research Ethics Committee).

mTOR and htt Immunoprecipitation Assays

Brain tissue was homogenized using an insulin syringe in ice-cold immunoprecipitation (IP) buffer containing: (1) For

mTOR IP: 40 mM Hepes (pH 7.5), 150 mM NaCl, 10 mM sodium pyrophosphate, 10 mM sodium glycerophosphate, 1 mM EDTA, 0.3% 3-[(3-cholamidopropyl) dimethylammonio]-1-propanesulfonate (CHAPS), 1 mM $NaVO_4$, 2.5 mM NaF, 2 mM PMSF, and 1:10.000 protease inhibitor cocktail (Sigma-Aldrich). (2) For htt IP: 50 mM Tris-HCl, pH = 8.0, 150 mM NaCl, 1% IGEPAL, 2 mM PMSF, 2.5 mM NaF, 1 mM $NaVO_4$, and 1:1000 protease inhibitor cocktail (Sigma-Aldrich). Protein (200 μg for mTOR IP and 300 μg for htt IP) was incubated overnight at 4 °C on a rotary mixer with 5 μg of anti-mTOR antibody (1 μl/50 μg protein; Cell Signaling), anti-htt antibody (MAB2166 or EM48, 1 μg/ul), or rabbit IgGs (Jackson Immunoresearch) as a negative control. The immune complexes were precipitated overnight at 4 °C with the addition of 5% A-Sepharose Cl-4B (Sigma-Aldrich). Beads were collected by centrifugation (5 min, 6000 rpm at 4 °C) and washed with (1) for mTOR IP: IP buffer three times and once with wash buffer containing [50 mM Hepes (pH = 7.5), 40 mM NaCl, 2 mM EDTA]. (2) For htt IP: with IP buffer, IP buffer-Phosphate buffered saline (PBS) (1:1) and PBS. Then, the samples were boiled for 7 min at 100 °C in SDS sample buffer. Immunocomplexes were resolved on 8% SDS-PAGE and analyzed by WB.

Cell Cultures, Transfection and Quantification of Cell Death

Conditionally immortalized wild-type $STHdh^{7Q/7Q}$ striatal neuronal progenitor cell line expressing endogenous levels of wild-type htt with 7 glutamines was obtained from wild-type $Hdh^{Q7/7}$ embryos at embryonic day 14. These cells were immortalized with SV40 antigen. Culture conditions were as described elsewhere [33]. Cells were transfected with scramble (1864, Addgene) or shRictor plasmids (21341; Addgene) at 50% of confluence using lipofectamine 2000 (Invitrogen, Carlsbad, CA, USA) as instructed by the manufacturer. Since both plasmids used confer resistance to puromycin, transfected cells were selected by adding this antibiotic to the medium 24 h after transfection. Once the cells stably expressed the plasmids, they were transfected with plasmids expressing human exon-1 htt, with 16 or 94 CAG repeats, tagged with the CFP [34]. For Rictor overexpression experiments, cells were transfected with human exon-1 htt plasmids (16 or 94 CAG repeats) together with empty myc (19400, Addgene) or myc-Rictor (11367, Addgene) expressing plasmids and analyzed 60 h later. To analyze cell death, cells were washed twice with PBS, fixed with 4% paraformaldehyde in PBS for 10 min, washed twice in PBS, and stained with Hoechst 33,258 (1 μg/ml; Molecular Probes, Inc.) for 5 min. After washing twice with PBS, the coverslips were mounted with mowiol. Nuclear DNA staining was observed with a fluorescence microscope (Olympus). Condensed or fragmented nuclei were considered apoptotic. At least 200 cells were evaluated for each condition, in each independent experiment. All the analyses were performed in a blinded fashion.

AAV-Mediated shRictor Expression Vectors

To knockdown Rictor expression, we designed a siRNA oligonucleotide targeting the mouse Rictor (5'GATCCGGC CAGTAAGATGGGAATCATTCTCGAGAATGATTCCCA TCTTACTGGCTTTTTGGA 3′). This siRNA was then used to obtain the corresponding shRNA to be cloned into a rAAV2/8-GFP adenoviral vector (BamHI site at 5′ and AgeI at the 3′). The rAAV2/8 plasmids and infectious AAV viral particles containing GFP expression cassette with SCB shRNA or Rictor shRNA were generated by the *Unitat de Producció de Vectors* from the Center of Animal Biotechnology and Gene Therapy at the Universitat Autònoma de Barcelona, Catalonia.

Intrastriatal Injection of Adeno-Associated Vectors

Six-week-old wild-type and R6/1 mice were deeply anesthetized with a mixture of oxygen and isofluorane (4–5 induction and 1–2 maintaining) and placed in a stereotaxic apparatus for bilateral intrastriatal injections of rAAV2/8 expressing shRictor or control shRNA (2 μl; 1.53×10^9 genomic copies). Two injections were performed in the striatum at the following coordinates relative to bregma: (1) anteroposterior (AP), + 0.8; mediolateral (ML), + 1.8; and 2.9 mm and (2) AP, + 0.3; ML, + 2; and 3 mm, below the dural surface with the incisor bar at 3 mm above the interaural line. Viral vectors were injected using a 10 μl-Hamilton microliter syringe at an infusion rate of 200 nl/min. The needle was left in place for 5 min to ensure complete diffusion of the viruses and then slowly retracted from the brain. Both hemispheres were injected with the same shRNA. Four weeks after injection, motor coordination was evaluated.

For immunohistochemistry, animals were deeply anesthetized with pentobarbital (60–80 mg/kg) and intracardially perfused with a 4% paraformaldehyde solution in 0.1 M sodium phosphate, pH 7.2. Brains were removed and post-fixed for 2 h in the same solution, cryoprotected with 30% sucrose in PBS with 0.02% sodium azide, and frozen in dry-ice cooled 2-methylbutane.

Accelerating Rotarod and Balance Beam

Accelerating rotarod was performed as described elsewhere [35] with a brief modification, performing three trials per day instead of 4. Balance beam was performed as described elsewhere [36].

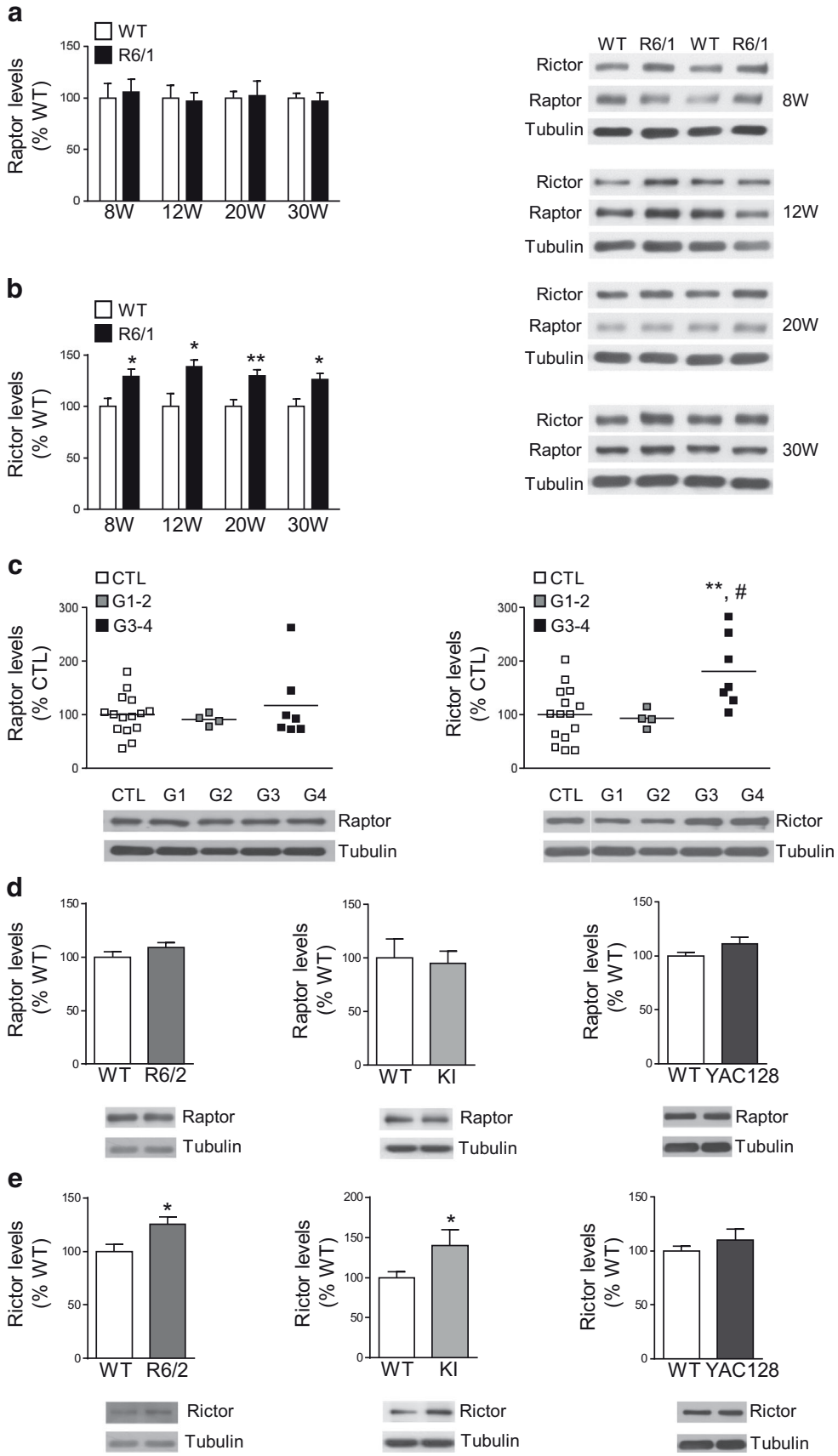

◀ **Fig. 1** Rictor, but not Raptor, levels are increased in the striatum of HD. Raptor (**a**, **c**) and Rictor (**b**, **d**) protein levels were analyzed by WB in protein extracts obtained from **a**, **b** the striatum of wild-type (WT) and R6/1 mice and from the putamen of HD patients at different stages of the disease progression (W, weeks; G1-G4, Vonsattel grades) and unaffected individuals (CTL), and **c**, **d** from the striatum of 16-week-old R6/2, 12-month-old $Hdh^{Q111/Q111}$, 18–19-month-old YAC128 mice and their corresponding WT mice. The graphs show **a** Raptor protein levels in R6/1 mice striatum and in the putamen of HD patients with respect to their controls at different stages of the disease progression, **b** Rictor protein levels in R6/1 mice striatum and in the putamen of HD patients with respect to their controls at different stages of the disease progression, **c** Raptor and **d** Rictor protein levels in R6/2, $Hdh^{Q111/Q111}$ and YAC128 mice striatum with respect to their controls. Values (obtained by densitometric analysis of WB data; Raptor or Rictor/α-tubulin ratio) are expressed as percentage of their corresponding controls (WT mice striatum for HD mouse models and the putamen of unaffected individuals for HD patients) and shown as mean ± SEM ($n = 6$–12 for R6/1 mice, R6/2, YAC128 mice, and their respective WT mice; $n = 3$ for $Hdh^{Q111/Q111}$ and their respective WT mice). Representative immunoblots are shown. *$P < 0.05$; **$P < 0.01$ as compared with respective WT mice (Student's t test); **$P < 0.01$ as compared with unaffected individuals; #$P < 0.05$ as compared with Vonsattel grade 1–2 HD patients (one-way ANOVA with Bonferroni's as a *post hoc* test)

Protein Extraction, Cellular Fractionation and WB Analyses

Animals were sacrificed at different ages by cervical dislocation. Brains were quickly removed and the striatum and cortex were dissected out and homogenized in lysis buffer. Protein extraction (for brain tissue and cell cultures), subcellular fractionation and WB analyses were performed as described elsewhere [37]. See primary antibodies used in supplementary Table S2. Incubation with mouse monoclonal antibodies against α-tubulin (α-tubulin antibody; 1:50,000; Sigma, St. Louis, MO, USA), actin (actin antibody; 1:20,000; MP Biomedicals, Aurora, OH, USA) or GAPDH (GAPDH antibody; 1:1000; Millipore; Massachusetts, CA, USA) was performed to obtain loading controls. After primary antibody incubation, membranes were washed with TBS-T and incubated for 1 h at room temperature with the appropriated horseradish peroxidase-conjugated secondary antibody (1:2000; Promega, Madison, WI, USA), and the reaction was finally visualized with the Western Blotting Luminol Reagent (Santa Cruz Biotechnology, Santa Cruz, CA, USA). WB replicates were scanned and quantified using a computer-assisted densitometrer (Gel-Pro Analyzer version 4, Media Cybernetics).

Immunohistochemistry

Coronal brain sections (30 μm) were obtained and processed as described elsewhere [38]. Free-floating brain sections were incubated overnight at 4 °C with anti-mTOR (1:500; Cell Signaling) anti-GFP (1:150; Abcam) or anti cleaved caspase-3 (1:200; Cell Signaling). Nuclei were stained with Hoechst 33258 (1:4000; Invitrogen, prepared in Tris-buffered saline (TBS)) and mhtt with the EM48 antibody (1:150; Millipore). Then, sections were washed in PBS and incubated 2 h at room temperature with the corresponding fluorescent secondary antibodies: Cy3 anti-rabbit (1:200) and Cy2 anti-mouse (1:200) both from Jackson ImmunoResearch. Tissue sections were examined by confocal microscopy using a TCS SL laser scanning confocal spectral microscope (Leica Microsystems Heidelberg) with argon and HeNe lasers attached to a DMIRE2 inverted microscope (Leica Microsystems Heidelberg). Images were taken with a 63× numerical aperture objective with a 2.5× digital zoom and standard pinhole (1 airy disk). Cleaved caspase-3 positive cells were visualized with a fluorescence microscope (Olympus) and counted in at least seven slices for each mouse. All cleaved caspase-3-positive cells present in the striatum were counted except those localized in the trajectory of the needle because we considered that these cells were positive due to the mechanical stress of the surgery procedure.

Statistical Analysis

All the results were expressed as the mean ± SEM. Statistical analysis was performed using the Student's t test or the one- or two-way ANOVA, followed by Bonferroni's post hoc test as appropriate and indicated in the figure legends. A 95% confidence interval was used and values of $p < 0.05$ were considered as statistically significant.

Results

Rictor Levels Are Increased in the Striatum of HD

Raptor and Rictor give substrate specificity to mTORC1 and mTORC2, respectively [1]. Thus, to investigate whether these two mTOR pathways could be altered in HD, we analyzed their levels by Western blot (WB) in the striatum of R6/1 mouse (expressing N-terminal exon-1 mhtt and with early onset of motor symptoms; [39]) and in the putamen of HD patients at different stages of the disease. In comparison with levels in aged-matched wild-type mice striatum, R6/1 displayed increased levels of Rictor, but not Raptor, in all the disease stages analyzed (Fig. 1a, b). In the putamen of HD patients, we detected increased levels of Rictor but only at late stages of the disease (Vonsattle grades 3 and 4) (Fig. 1a, b). Interestingly, this effect was specific for the striatum, since we did not detect changes in the cortex of R6/1 mice neither in the cortex of affected individuals (Supplementary Fig. S1).

Next, we analyzed whether these alterations are a common feature in striatal cells expressing different forms of mhtt. To

this end, we analyzed Raptor and Rictor levels in the striatum of R6/2 mice, which express N-terminal exon-1 mhtt and show earlier onset and more severe symptoms than R6/1 mice [39], $Hdh^{Q111/Q111}$ and YAC128 mice, which express full-length mhtt and show late onset and slow progression of the disease [32, 40]. Our results show that in comparison with their corresponding controls 16-week-old R6/2 and 12-month-old $Hdh^{Q111/Q111}$ display increased levels of Rictor, but not Raptor, whereas no changes were detected in 18–19-month-old YAC128 mice striatum (Fig. 1c, d). Thus, since Rictor levels have been previously shown to regulate mTORC2 activity [41–46], our results suggest that mTORC2 activity could be increased in the striatum of HD. However, a previous study suggested that mTOR is sequestered in mhtt aggregates, hampering its activity [19]. Therefore, we analyzed whether mTOR interact with mhtt in R6/1 mice striatum. First of all, we analyzed mTOR localization by WB in nuclear and cytoplasmic enriched fractions obtained from the putamen of HD patients and from the striatum of 30-week-old wild-type and R6/1 mice, and also by immunohistochemistry in the striatum of R6/1 mice. We found that mTOR was mainly restricted to the cytoplasmic compartment in both human putamen (Fig. 2a) and R6/1 mice striatum (Fig. 2b), and, moreover, we failed to detect any co-localization between mTOR and EM48-positive mhtt aggregates in R6/1 mice striatum (Fig. 2b). Furthermore, in 30-week-old wild-type and R6/1 mice striatum, we observed that mTOR did not co-immunoprecipitate with mhtt (Fig. 2c), whereas p62, used as a positive control, co-immunoprecipitated with mhtt (Supplementary Fig. S2) as previously described [38]. In addition, mTOR was detected in the

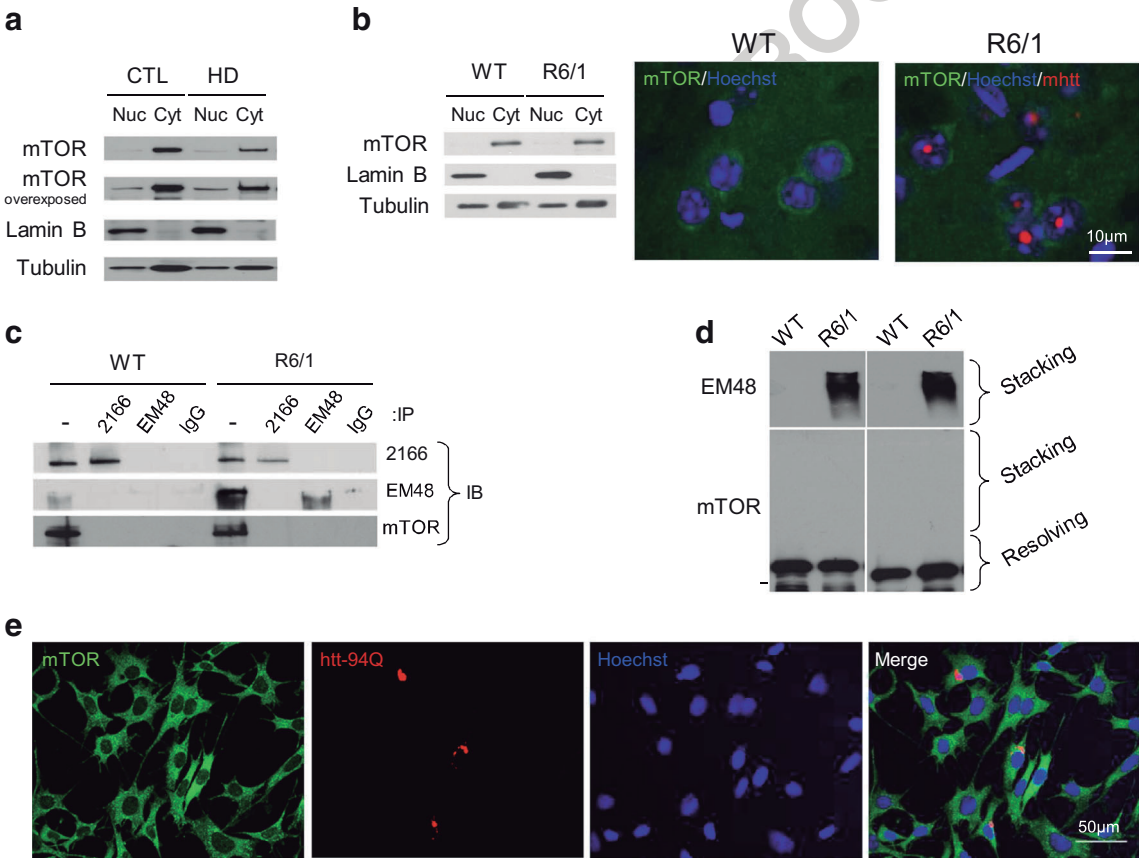

Fig. 2 mTOR is mainly localized in the cytoplasm of striatal cells. Localization of mTOR was determined by WB of nuclear (Nuc; loading control lamin B) and cytoplasmic (Cyt; loading control α-tubulin) enriched fractions obtained **a** from unaffected individuals (CTL) and Vonsattel grade 3–4 HD patients (HD), and **b** from 30-week-old wild-type (WT) and R6/1 mice striatum. Representative immunoblots are shown. **b** mTOR (green) was analyzed by immunohistochemistry in the striatum of wild-type (WT) and R6/1 mice at 30 weeks of age. Nuclei were stained with Hoechst 33258 (blue) and mhtt with the EM48 antibody (red). Merged images show that mTOR does not co-localize with EM48-positive intra-nuclear inclusions. Scale bar 10 μm. **c** Interaction of mTOR and htt was analyzed in WT and R6/1 mice striatum at 30 weeks of age by immunoprecipitation (IP). Wild-type htt was immunoprecipitated with the 2166 antibody, mhtt with the EM48 antibody and mouse IgGs were used as control. Membranes were then subjected to immunoblotting (IB) with different antibodies as indicated in the representative immunoblot. – indicates total protein extract. **d** The presence of mhtt and absence of mTOR in stacking gels from WBs of samples obtained from 30-week-old WT and R6/1 mice striatum. mTOR was also analyzed WB in the resolving gel. **e** Representative images illustrate $STHdh^{Q7/Q7}$ cells 72 h after transfection with a plasmid expressing exon-1-encoded N-terminal htt with 94 glutamines fused to CFP (htt-94Q; red). Nuclei were stained with Hoechst 33,258 (blue) and endogenous mTOR was stained by immunocytochemistry (green). Merged images show that mTOR does not co-localize with mhtt intra-nuclear aggregates. Scale bar 50 μm

resolving gel at the expected molecular weight, whereas mhtt was detected in the stacking gel by using the EM48 antibody (Fig. 2d). Finally, in striatal cells overexpressing N-terminal htt with 94 glutamines, we failed to detect co-localization between mTOR and mhtt aggregates (Fig. 2e). Altogether, these results indicate that mTOR does not interact/co-localize with mhtt aggregates and thus it can be functionally active in striatal cells.

Increased Rictor Levels Correlate with Increased mTORC2 Signaling in the Striatum of HD

To explore whether elevated Rictor levels translated to an increased interaction with mTOR, we examined the association of Rictor/Raptor with mTOR in the striatum of 20-week-old wild-type and R6/1 mice by immunoprecipitation. We observed that both proteins co-immunoprecipitated with mTOR but the amount of co-immunoprecipitated Rictor was higher in R6/1 than in wild-type mice striatum (Fig. 3a). In contrast, no alterations in the levels of Raptor or Rictor interaction with mTOR were detected in the cortex of R6/1 mice (Supplementary Fig. S3). Increased interaction mTOR/Rictor has been postulated as a good read-out for increased mTORC2 pathway signaling. Thus, to evaluate the kinase activity of mTOR we next analyzed by WB the levels of two phosphorylated forms of mTOR: (1) pSer2448, which is phosphorylated by Akt and S6K to increase mTOR activity [47, 48]) and (2) pSer2481, which is an auto-phosphorylation event that serves to monitor mTOR catalytic activity [49]. Interestingly, our results show increased levels of both mTOR phosphorylated forms in the striatum of R6/1 mice from 12 weeks of age onwards (Fig. 3b). In addition, pSer2481 mTOR levels were significantly increased in the putamen of Vonsattel grade 3–4 patients, whereas pSer2448 mTOR protein levels tended to increase although differences did not reach statistical significance (Fig. 3c). In contrast, no changes in pSer2448 mTOR and pSer2481 mTOR levels were observed in the cortex of HD (Supplementary Fig. S4) nor in total mTOR levels in any of the conditions analyzed (Supplementary Fig. S5). In accordance with increased kinase activity of mTORC2, pSer473 Akt levels were increased in the striatum of R6/1 mice, while no differences were observed in pSer389 S6K (Fig. 3d), pSer757 Ulk1 (Supplementary Fig. S6a), and total Akt, S6K, and Ulk1 levels (Supplementary Fig. S6b), suggesting a specific overactivation of the mTORC2 pathway in the striatum of HD. Accordingly, the levels of phospho-Thr246 proline-rich Akt substrate 40 kDa (PRAS40), a substrate of pAkt [50], was increased in the striatum of R6/1 mice at 20 and 30 weeks of age (Supplementary Fig. S6c). In addition, and in good correlation with increased Rictor levels, we detected enhanced pSer473 Akt and unchanged pSer389 S6K levels in the striatum of R6/2 and $Hdh^{Q111/Q111}$ mice whereas pSer473 Akt levels were not altered in YAC128 mice striatum (Fig. 3). Furthermore, and according with no changes in pmTOR nor in Rictor/mTOR co-immunoprecipitation, pSer473 Akt levels were not altered in the cortex of R6/1 mice at any of the ages analyzed (Supplementary Fig. S7). Taken together, these results suggest an increased mTORC2 activity specifically in HD striatum.

mTORC2 Activity Contributes to Prevent Mhtt-Induced Cell Death In Vitro

So far, our results suggest an increased mTORC2 activity in the striatum of HD that could be responsible, in part, for the augmented pSer473 Akt levels in the striatum of HD mouse models [26, 27], which we suggested may delay mhtt-induced cell death [27]. To test our hypothesis, we down- or upregulated Rictor in striatal cells expressing wild-type or mhtt. To downregulate Rictor, we generated $STHdh^{Q7/Q7}$ cells, stably expressing shRNA against Rictor (shRictor). Cells stably expressing scrambled sequence (shSCB) were used as control. These stable cell lines were then transfected with exon-1 htt plasmids with 16 (wild-type) or 94 (mutant) glutamines (Q) fused to cyan fluorescent protein (CFP) [51]. To overexpress Rictor, $STHdh^{Q7/Q7}$ cells were co-transfected with myc-Rictor or myc-only plus wild-type or mhtt-expressing plasmid [4]. Protein levels of mTOR, Rictor, Raptor, and phosphorylated levels of downstream targets of mTORC1 and mTORC2 were analyzed by WB 60 h after transfection. As expected, wild-type and mhtt-expressing cells stably expressing shRictor displayed decreased Rictor protein levels when compared with cells stably expressing shSCB (Fig. 4a). In these cells, mTORC2 signaling was inhibited, as indicated by decreased levels of pSer473 Akt, whereas there was no discernible effect on mTORC1 activity as we found no changes in the levels of the mTORC1 target pThr389 S6K (Fig. 4a). $STHdh^{Q7/Q7}$ cells transfected with wild-type or mhtt plus myc-Rictor expressing plasmids showed increased Rictor and pSer473 Akt protein levels while pThr389 S6K levels were not altered in comparison with cells transfected with myc-only expressing plasmids (Fig. 4b). Total protein levels of mTOR, Akt, and S6K were similar in all the conditions analyzed (Supplementary Fig. S8). Next, we analyzed the effect of silencing or overexpressing Rictor on the survival of $STHdh^{Q7/Q7}$ cells transfected with wild-type or mhtt. Overexpression of mhtt increased the percentage of apoptotic cells in comparison to cells overexpressing wild-type htt (Fig. 4c, d). The percentage of apoptosis was further increased in mhtt-expressing cells in which Rictor levels were reduced (Fig. 4c) while overexpression of Rictor in $STHdh^{Q7/Q7}$ cells prevented mhtt-induced cell death (Fig. 4d). In summary, our results show that Rictor is playing a neuroprotective role in the presence of mhtt.

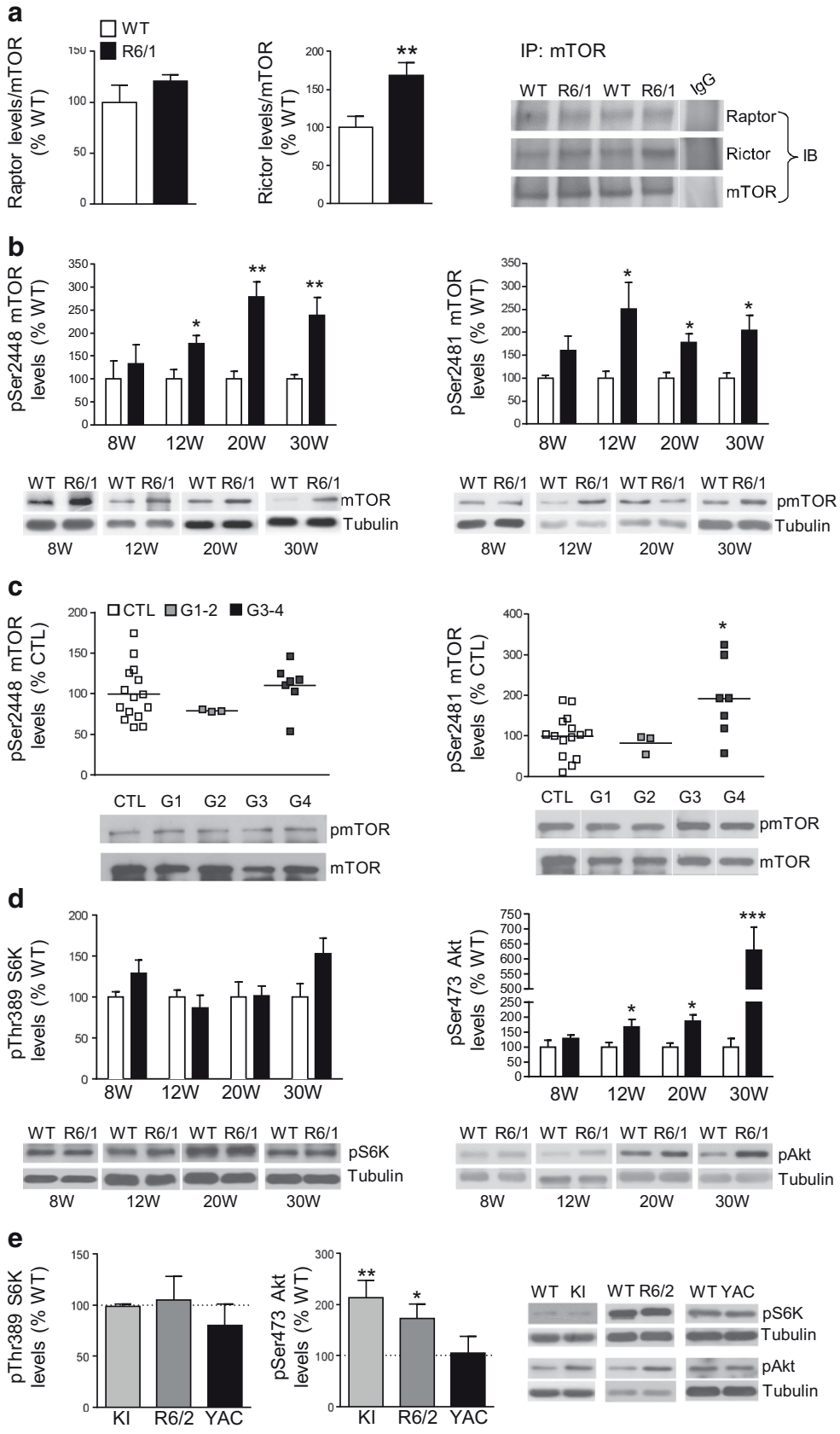

◀ **Fig. 3** mTORC2 activity is increased in HD striatum. **a** Interaction of Raptor and Rictor with mTOR was analyzed in protein extracts from 20-week-old WT and R6/1 mice striatum by immunoprecipitation (IP). mTOR was immunoprecipitated and then the membranes were subjected to immunoblotting (IB) as indicated. The graphs show Raptor and Rictor protein levels immunoprecipitated with mTOR in R6/1 respect to WT mice striatum. **b**, **c** Graphs show pSer2448 and pSer2481 mTOR protein levels analyzed by WB in protein extracts from the striatum of wild-type (WT) and R6/1 mice (**b**) and from the putamen of an unaffected individuals (CTL) and HD patients (**c**) at different stages of the disease progression (W, weeks; G1-G4, Vonsattel grades). **d**, **e** Graphs show pSer389 S6K and pSer473 Akt protein levels analyzed by WB in protein extracts obtained from **d** the striatum of WT and R6/1 mice at different stages of the disease progression and **e** of 16-week-old R6/2, 12-month-old $Hdh^{Q111/Q111}$, 18–19-month-old YAC128 mice and their corresponding WT mice. Representative immunoblots are shown for each experiment. Values were obtained by densitometric analysis of WB data and are expressed as percentage of WT mice (**a**, Raptor or Rictor/mTOR; **b**, pSer2448 mTOR or pSer2481 mTOR/α-tubulin ratio; **d** and **e**, pSer389 S6K or pSer473 Akt/α-tubulin, ratio) or of unaffected individuals (**c**, pSer2448 mTOR or pSer2481 mTOR/α-tubulin ratio) and expressed as mean ± SEM (**a**, $n = 5–7$; **b**, $n = 6$; **d** and **e**, $n = 6$ for R6/1 and YAC128 mice and their respective WT mice; $n = 5$ for R6/2 and their respective WT mice and $n = 4$ for $Hdh^{Q111/Q111}$ and their respective WT). $^{*}P < 0.05$; $^{**}P < 0.01$; $^{***}P < 0.001$ as compared with WT mice in **a**, **b**, **d**, and **e**, Student's *t* test and $^{*}P < 0.05$ as compared with unaffected individuals, one-way ANOVA with Bonferroni's as a *post hoc* test

Rictor Knockdown Worsens Motor Behavior in Presymptomatic R6/1 Mice

Results obtained so far indicate that mTORC2 activity is increased in R6/1 mice striatum, possibly due to increased Rictor levels, and in vitro experiments suggest that Rictor levels modulate cell survival against mhtt toxicity. Thus, we asked whether blocking the increase in Rictor levels in R6/1 striatum could worsen motor symptoms. For this purpose, 6-week-old WT and R6/1 mice were bilaterally injected with AAV-shSCB or AAV-shRictor into the striatum, and behavior was assessed 4 weeks after the injection (Fig. 5a). Motor learning and coordination were evaluated by the accelerating rotarod and balance beam tests, respectively. Knockdown of Rictor worsened motor learning deficits in R6/1 mice, evaluated by the latency to fall in the accelerating rotarod (Fig. 5b). Alterations in motor coordination that could not yet be observed at this stage of the disease in R6/1 mice injected with AAV-SCB were observed in R6/1 mice injected with AAV-shRictor (Fig. 5c), indicating a worsening of the disease phenotype and suggesting that increased Rictor levels in R6/1 mice striatum could improve neuronal function. After the behavioral tests, striata were processed for WB and immunohistochemistry analyses. Rictor levels were not altered in wild-type mice but were normalized to wild-type levels in R6/1 mice striatum although we did not detect alterations in pSer473Akt levels (Fig. 5d). In order to better analyze the consequences of knocking down Rictor, we analyzed SGK levels since it has been shown that Rictor regulates SGK degradation [52]. According to this, we observed increased levels of SGK both in wild-type and R6/1 mice striatum injected with AAV-shRictor (Fig. 5d). In addition, Raptor, mTOR, Akt, S6K, and pThr389 S6K levels were not modified after Rictor silencing in wild-type and R6/1 mice striatum (Supplementary Fig. S9). Finally, we analyzed the number of caspase-3 positive cells and observed that Rictor knockdown increased their number only in R6/1 mice striatum (Fig. 5e).

Discussion

The present study shows that Rictor levels are specifically increased in the striatum of HD possibly contributing to counteract mhtt toxicity, at least temporarily, improving striatal neurons function.

Here, we show that Rictor levels were specifically increased in the striatum of HD mouse models and in the putamen of HD patients at late stages of the disease, whereas Raptor levels were not altered. Rictor expression has been shown to be regulated by miR-218 in oral squamous carcinoma cells [53] and in medulloblastoma cells [54]. Binding of a miRNA to its target mRNA results in its repression [55]. Interestingly, miR-218 is decreased in the striatum of 10-week-old R6/2 mice [56] and in the putamen of Vonsattel grade 4 patients [57] and it is not altered in the motor cortex of HD patients at any of the Vonsattel stages [58]. Therefore, decreased repression of Rictor mRNA expression, due to decreased levels of miR-218, could account for increased Rictor protein levels in the striatum of HD mouse models and in the putamen of HD patients at late stages of the disease. Interestingly, increased Rictor expression has also been detected in blood from 16-week-old R6/2 mice [59], which suggests changes in Rictor levels as a possible biomarker of the disease.

Augmented levels of Rictor can result in enhanced mTORC2 activity [41–46]. However, in contrast to our results, it was proposed that mTOR is inactivated in HD based on the observation that mTOR gets sequestered into both nuclear and cytoplasmic mhtt aggregates [19]. Our results indicate that mTOR does not interact with mhtt aggregates in the striatum of R6/1 mice and in a striatal cell line or in HD patients as indicated by (1) predominant localization of mTOR in the cytoplasm, (2) lack of interaction between mTOR and mhtt by immunoprecipitation, (3) absence of mTOR in the stacking gel, and (4) no co-localization of mTOR with mhtt in striatal cells transfected with exon-1 mhtt. Differences between the results by Ravikumar et al. [19] and our study could be related to the fact that they analyzed a different mouse model, the N171-82Q mice. In fact, contradictory results have been obtained when analyzing mTOR activity in the striatum of these mice since both decreased [18] and increased [17] activity has been reported.

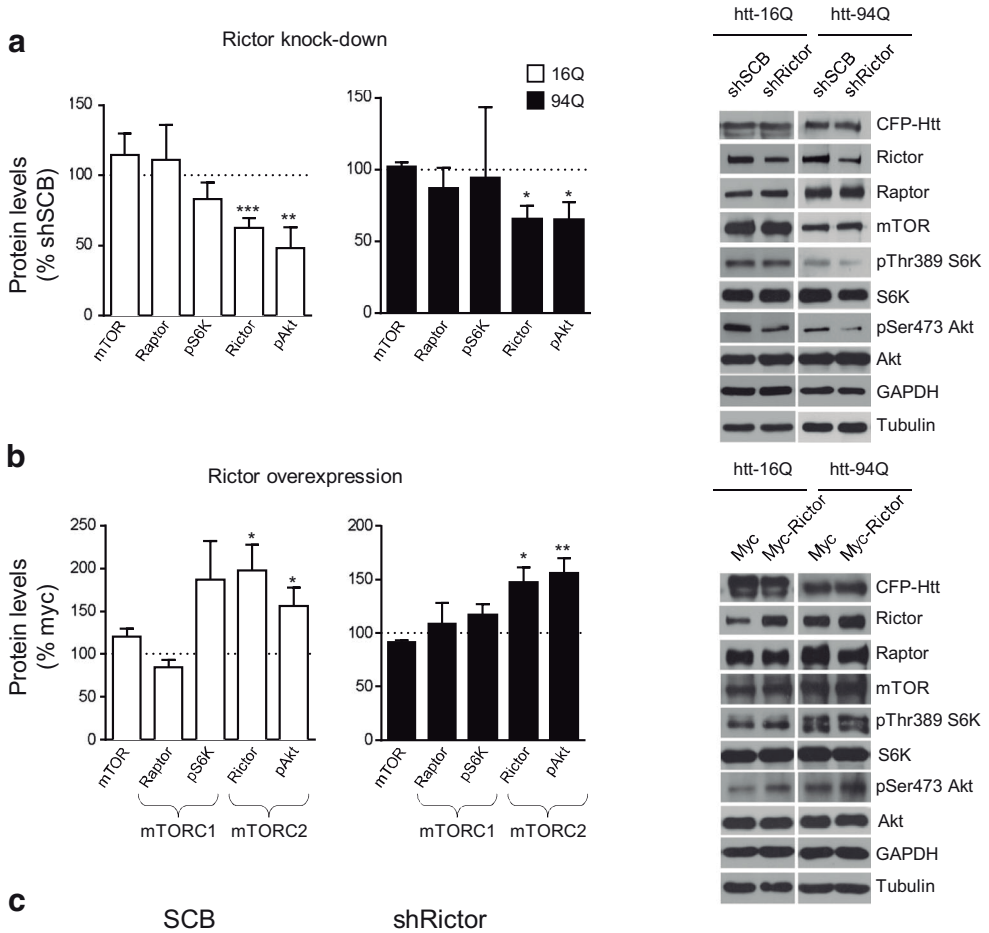

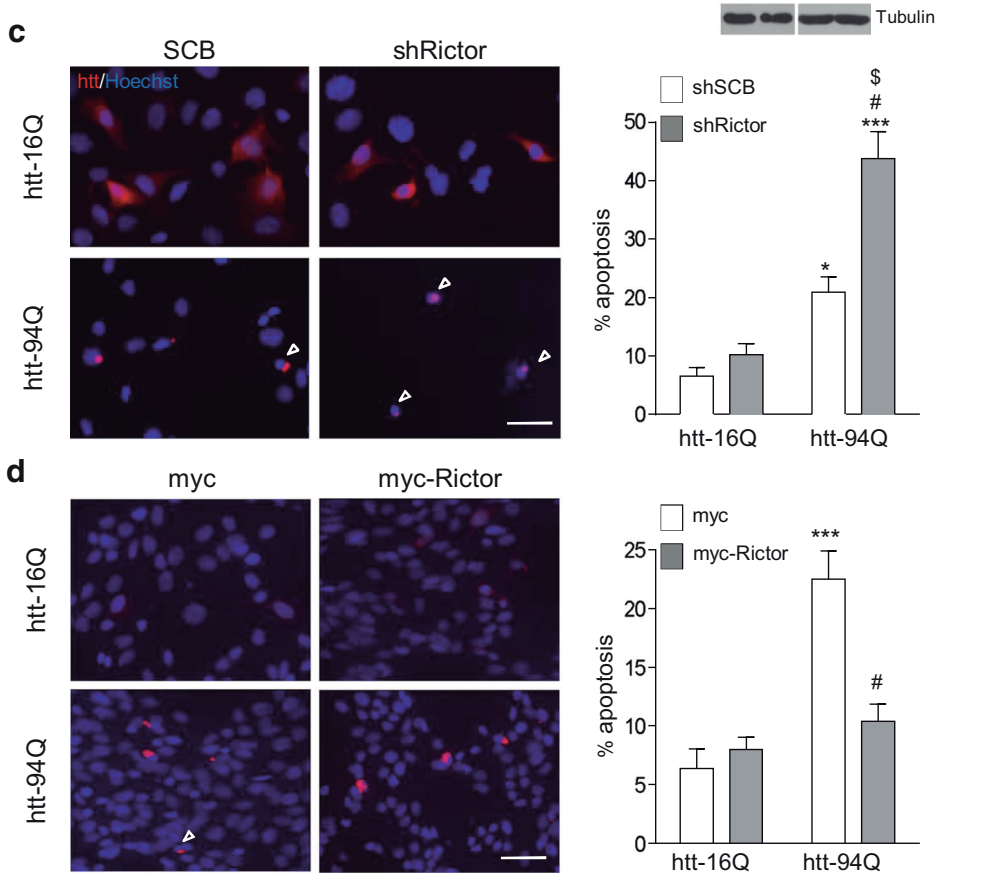

◀ **Fig. 4** Rictor levels modulate mhtt-induced cell death in vitro. Protein levels of mTOR, Raptor, Rictor, mTORC1 (pThr389 S6K), and mTORC2 (pSer473 Akt) targets were analyzed by WB of protein extracts obtained from STHdh$^{Q7/Q7}$ cells transfected with wild-type (htt-16Q) or mhtt (htt-94Q) plus (**a**) shSCB or shRictor or (**b**) plus myc-only or myc-Rictor expressing plasmids. Tubulin and GAPDH were used as loading control. Representative immunoblots are shown. Values (obtained by densitometric analysis of WB data) are expressed as percentage of control cells (transfected with htt-16Q plus shSCB or myc-only expressing plasmids; mTOR, Raptor, Rictor, pThr389 S6K and pSer473 Akt/α-tubulin ratio) and shown as mean ± SEM of four experiments performed in independent cultures. $*P < 0.05$, $**P < 0.01$ compared with control cells. Student's *t* test. Representative images illustrate **c** STHdh$^{Q7/Q7}$ cells stably expressing shSCB or shRictor transfected with htt-16Q-CFP or htt-94Q-CFP expressing plasmids and **d** STHdh$^{Q7/Q7}$ cells co-transfected with htt-16Q-CFP or htt-94-CFP expressing plasmids plus myc-only or myc-Rictor expressing plasmids. Nuclei were stained with Hoechst 33258. Arrowheads show apoptotic nuclei. Scale bar, 20 μm. Graphs show the percentage of apoptotic nuclei in **c** cells expressing htt-16Q or htt-94Q plus shSCB or shRictor and **d** cells expressing htt-16Q or htt-94Q plus myc-only or myc-Rictor expressing plasmids, normalized to the total number of cells transfected with wild-type or mutant htt. Data are represented as mean ± SEM of three independent experiments (200–400 nuclei were examined in each condition for every experiment). $*P < 0.05$ and $***P < 0.001$ compared with htt-16Q + shSCB transfected cells; $\#P < 0.001$ compared with htt-16Q + shRictor transfected cells; $^{\$}P < 0.01$ compared with htt-94Q + shSCB transfected cells (Two-way ANOVA followed by Tukey post hoc test)

Our results show an increase in Rictor/mTOR interaction in the striatum of R6/1 that could indicate augmented mTORC2 activity as previously shown [41–46]. In addition, we show that phosphorylation of mTOR at Ser2481 and Ser2448 is increased in the striatum of R6/1 mice from 12 weeks of age onwards. Phosphorylation at Ser2481 is the result of an autophosphorylation and it serves as a biomarker of intrinsic mTOR catalytic activity [49]. Indeed, we observed that phosphorylated levels of the mTORC2 target Akt are increased in the striatum of those HD mouse models that showed increased levels of Rictor. Previous results have shown that alterations in Rictor levels could impact on mTORC1 activity. Knockdown of Rictor in *Tsc2*$^{-/-}$ cells results in increased S6 K1 phosphorylation and overexpression of Rictor in HEK293 cells increases its association with mTOR and decreases the association of Raptor with mTOR, thus affecting mTORC1 activity [43]. Furthermore, Akt signals to mTORC1 by phosphorylating PRAS40, an mTORC1 inhibitor, causing its dissociation from Raptor and thus activating mTORC1 [60–62]. In fact, our results show that phosphorylated levels of PRAS40 were increased in R6/1 mice striatum in correlation with enhanced Akt activity. However, although Rictor, and Rictor-mTOR interaction levels were increased in the striatum of R6/1 mice, Raptor-mTOR interaction was not altered, nor the phosphorylation levels of S6K and Ulk1, thus suggesting that mTORC1 activity is not altered in striatal cells expressing mhtt. Therefore, there might be intrinsic cellular properties that modify the effect of Rictor overexpression on mTORC1 complex activity being stronger in some cell types or experimental conditions than in others.

In accordance with increased Rictor levels leading to an enhancement of mTORC2 activity in HD striatum with no changes in mTORC1 activity, we observed that, in an in vitro context, Rictor knockdown in striatal cells expressing mhtt resulted in a decrease in the phosphorylation of Akt, without alteration in phospho-S6K levels. Our results agree with previous studies showing that silencing of Rictor in neural or endothelial cells only affects mTORC2 activity [9, 16, 63–67]. Interestingly, and similarly to what we detected in the striatum of HD mouse models, overexpression of Rictor in striatal cells expressing mhtt only affected mTORC2 activity. Controversially, we found that Rictor knockdown in the striatum of wild-type and R6/1 mice did not decrease pSer473Akt levels. In contrast, decreased Rictor levels resulted in an increase of SGK levels, both in wild-type and R6/1 mice striatum, which is in agreement with the fact that Rictor regulates SGK degradation [52], indicating that downregulation of Rictor in the striatum has consequences on its functions. However, increased levels of SGK have been shown to be neuroprotective for injured neurons [68, 69] and therefore these changes cannot explain the alterations in R6/1 mice behavior induced by Rictor knockdown. Taken together, these observations suggest the idea that, in the presence of mhtt, Rictor might regulate neurons function in an Akt-independent manner. Indeed, Rictor functions independently of Akt have been proposed [52, 70, 71]) such as for example the regulation of autophagy in epithelial cells from kidney [72]. Therefore, we cannot rule out that these unexplored roles of Rictor could play an important role in HD regulating neuronal function.

Here, we show that in striatal cells expressing mhtt Rictor knockdown increased, whereas overexpression of Rictor prevented, cell death. These results were extended in vivo as we observed the presence of few cleaved caspase-3-positive cells only in the striatum of R6/1 mice injected with AAV-shRictor, which suggests that alterations in behavior would be mostly related with neuronal dysfunction. In agreement, brains from Rictor knockout mice do not present enhanced cell death [16], reinforcing the idea that Rictor exert a crucial function in regulating not only de survival, but also the function, of brain cells against toxic stimuli such as, in this case, the presence of mhtt. Accordingly, increased Rictor levels were detected in those mouse models showing little, if any, neuronal death in the striatum [39, 40, 73]. Furthermore, and reinforcing the idea of a neuroprotective role of Rictor, its levels were not altered in YAC128 mice striatum, which show striatal cell death at the age analyzed [32]. Since striatal neurons are the most vulnerable to the presence of mhtt, our results could indicate that increased Rictor levels belong to a compensatory mechanism trying to counteract mhtt toxicity in these susceptible cells. Controversially, we detected increased

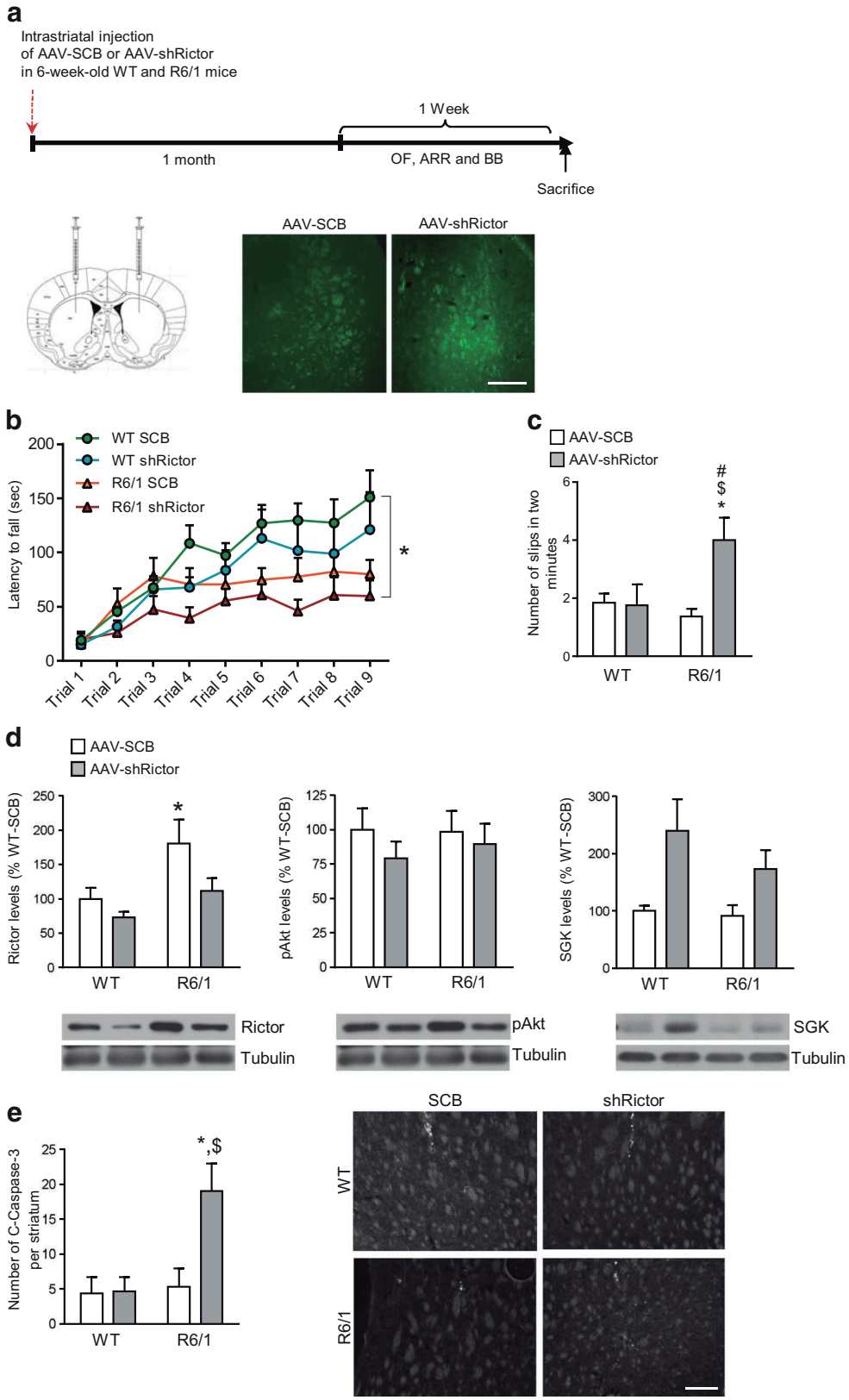

levels of Rictor in the putamen of HD patients only at late stages of the disease when most of the neurons have already died. Results obtained in mouse models suggest that the early increase of Rictor levels during disease progression could prevent cell death a posteriori. Thus, we propose that the increase of Rictor levels in the putamen of HD patients takes place too

◀ **Fig. 5** Intrastriatal injection of AAVs expressing shRictor worsens R6/1 mice phenotype. Six-week-old wild-type (WT) and R6/1 mice were injected bilaterally with AAV-shSCB or AAV-shRictor in the striatum. **a** Scheme showing the protocol used to normalize Rictor levels in R6/1 pre-symptomatic mice. Representative images, obtained by immunohistochemistry against GFP, show transduced striatal cells 4 weeks after the injections. Scale bar 400 μm. **b**, **c** Motor performance was addressed testing WT and R6/1 injected mice by accelerating rotarod (**b**) and balance beam (**c**) 4 weeks after the injections. The graphs represent the mean ± SEM ($n = 9$ per group). **d** Rictor, pSer473 Akt, and SGK protein levels were analyzed by WB of protein extracts obtained from WT and R6/1 mice striatum 5 weeks after the intrastriatal injection of AAVs. Graphs show protein levels with respect to control situation (striatum of WT mice injected with AAV-SCB). Values (obtained by densitometric analysis of WB data) are expressed as percentage of control (Rictor, pSer473 Akt, and SGK/α-tubulin ratio) and shown as mean ± SEM ($n = 9$). Representative immunoblots are shown. $^{*}P < 0.05$ compared to WT AAV-shSCB mice; $^{\$}P < 0.05$ compared to WT AAV-shRictor mice and $^{\#}P < 0.05$ compared to R6/1 AAV-shSCB mice. Data were analyzed by two-way ANOVA followed by Bonferroni as post hoc test. **e** Graph shows the number of cleaved caspase-3 (C-caspase-3)-positive cells in the striatum of all the conditions analyzed. Values are expressed as mean ± SEM ($n = 3$ animals/group). Representative images are shown. Scale bar 100 μm. $^{*}p < 0.05$ compared to WT AAV-shSCB mice; $^{\$}p < 0.05$ compared to WT AAV-shRictor mice and $^{\#}p < 0.05$ compared to R6/1 AAV-shSCB mice. Data were analyzed by two-way ANOVA followed by Bonferroni as post hoc test

late to compensate the detrimental effects caused by the presence of mhtt, and is not able to prevent cell death.

Rictor functions in the brain are beginning to be unraveled. It has been shown to modulate brain size, dendritic processes and synaptic plasticity [16, 64, 74], and alterations in its activity are involved in drug addiction [75] and schizophrenia [15]. Here, we show that Rictor seems to play a role in the regulation of neuronal function in the striatum of HD. Increased Rictor levels and, maybe mTORC2 activity, in the presence of mhtt suggest that neurons possess the ability to activate adaptive responses to counteract cell dysfunction and death in animal models. Understanding how and to what extent these neuroprotective pathways can be activated in the affected tissues would provide useful information for developing therapeutic tools. In this line, the maintenance of mTORC2 signaling could extend the time window for the application of therapies aimed to improve neuronal function and prevent striatal neurons death.

Acknowledgements We are very grateful to Drs. Saavedra and Azkona (University of Barcelona) for critical reading of the manuscript, Dr. Azkona for his advice on intrastriatal injection of AAVs, Dr. Lucas (Centre for Molecular Biology "Severo Ochoa," Madrid, Spain) for providing the plasmids expressing wild-type or mhtt fused to CFP, Dr. MacDonald (Massachusetts General Hospital, Boston, Massachusetts, USA) for the generous gift of STHdh$^{Q7/Q7}$ cell line and Hdh$^{Q111/Q111}$ mice, Dr. Hayden (Centre for Molecular Medicine and Therapeutics, Child and Family Research Institute, University of British Columbia, Vancouver, Canada) for providing the YAC 128 mice, and Dr. Bayascas for the generous gift of antibodies against phosphorylated and total PRAS40. We also thank the Neurological Tissue Bank of the Biobanc-Hospital Clinic-IDIBAPS (Barcelona, Spain) for providing human tissue samples, Ana López and Maria Teresa Muñoz for their technical support. This work was supported by the project PI13/01250 *integrado en el Plan Nacional de I+D+I y cofinanciado por el ISCIII-Subdirección General de Evaluación y el Fondo Europeo de Desarrollo Regional (FEDER)*, Ministerio de Economia y Competitividad (grants SAF2010-21058; CSD2008-00005, SAF2013-48983-R; SAF2013-45888R and SAF2016-08573-R), European Commission with a Marie Curie International Reintegration Grant (PIRG08-GA-2010-276957), Spain, funds obtained via the crowdfunding platform Goteo.org and sponsored by "Mememtum: early detection of neurological disorders," Portal d'Avall SL, the UTE project CIMA and a NARSAD Independent Investigator Award. R.A. is a fellow of Ministerio de Economia y Competitividad, Spain.

Compliance with Ethical Standards

All procedures were performed in compliance with the NIH Guide for the Care and Use of Laboratory Animals and approved by the local animal care committee of Universitat de Barcelona following European (2010/63/UE) and Spanish (RD53/2013) regulations for the care and use of laboratory animals.

Conflict of Interest The authors declare that they have no competing interests.

References

1. Laplante M, Sabatini DM (2012) mTOR signaling in growth control and disease. Cell 149:274–293
2. Jacinto E, Loewith R, Schmidt A, Lin S, Ruegg MA, Hall A, Hall MN (2004) Mammalian TOR complex 2 controls the actin cytoskeleton and is rapamycin insensitive. Nat Cell Biol 6:1122–1128
3. Kim DH, Sarbassov DD, Ali SM, King JE, Latek RR, Erdjument-Bromage H, Tempst P, Sabatini DM (2002) mTOR interacts with raptor to form a nutrient-sensitive complex that signals to the cell growth machinery. Cell 110:163–175
4. Sarbassov DD, Ali SM, Kim DH, Guertin DA, Latek RR, Erdjument-Bromage H, Tempst P, Sabatini DM (2004) Rictor, a novel binding partner of mTOR, defines a rapamycin-insensitive and raptor-independent pathway that regulates the cytoskeleton. Curr Biol 14:1296–1302
5. Zoncu R, Efeyan A, Sabatini DM (2011) mTOR: from growth signal integration to cancer, diabetes and ageing. Nat Rev Mol Cell Biol 12:21–35
6. Kim J, Kundu M, Viollet B, Guan KL (2011) AMPK and mTOR regulate autophagy through direct phosphorylation of Ulk1. Nat Cell Biol 13:132–141
7. Sarbassov DD, Guertin DA, Ali SM, Sabatini DM (2005) Phosphorylation and regulation of Akt/PKB by the rictor-mTOR complex. Science 307:1098–1101
8. Garcia-Martinez JM, Alessi DR (2008) mTOR complex 2 (mTORC2) controls hydrophobic motif phosphorylation and activation of serum- and glucocorticoid-induced protein kinase 1 (SGK1). Biochem J 416:375–385
9. Guertin DA, Stevens DM, Thoreen CC, Burds AA, Kalaany NY, Moffat J, Brown M, Fitzgerald KJ et al (2006) Ablation in mice of the mTORC components raptor, rictor, or mLST8 reveals that mTORC2 is required for signaling to Akt-FOXO and PKCalpha, but not S6K1. Dev Cell 11:859–871
10. Oh WJ, Jacinto E (2011) mTOR complex 2 signaling and functions. Cell Cycle 10:2305–2316

11. Costa-Mattioli M, Monteggia LM (2013) mTOR complexes in neurodevelopmental and neuropsychiatric disorders. Nat Neurosci 16:1537–1543
12. Lipton JO, Sahin M (2014) The neurology of mTOR. Neuron 84: 275–291
13. Sun YX, Ji X, Mao X, Xie L, Jia J, Galvan V, Greenberg DA, Jin K (2014) Differential activation of mTOR complex 1 signaling in human brain with mild to severe Alzheimer's disease. J Alzheimers Dis 38:437–444
14. Sharma A, Hoeffer CA, Takayasu Y, Miyawaki T, McBride SM, Klann E, Zukin RS (2010) Dysregulation of mTOR signaling in fragile X syndrome. J Neurosci 30:694–702
15. Siuta MA, Robertson SD, Kocalis H, Saunders C, Gresch PJ, Khatri V, Shiota C, Kennedy JP et al (2010) Dysregulation of the norepinephrine transporter sustains cortical hypodopaminergia and schizophrenia-like behaviors in neuronal rictor null mice. PLoS Biol 8:e1000393
16. Thomanetz V, Angliker N, Cloetta D, Lustenberger RM, Schweighauser M, Oliveri F, Suzuki N, Ruegg MA (2013) Ablation of the mTORC2 component rictor in brain or Purkinje cells affects size and neuron morphology. J Cell Biol 201:293–308
17. Pryor WM, Biagioli M, Shahani N, Swarnkar S, Huang WC, Page DT, MacDonald ME, Subramaniam S (2014) Huntingtin promotes mTORC1 signaling in the pathogenesis of Huntington's disease. Sci Signal 7:ra103
18. Lee JH, Tecedor L, Chen YH, Monteys AM, Sowada MJ, Thompson LM, Davidson BL (2015) Reinstating aberrant mTORC1 activity in Huntington's disease mice improves disease phenotypes. Neuron 85:303–315
19. Ravikumar B, Vacher C, Berger Z, Davies JE, Luo S, Oroz LG, Scaravilli F, Easton DF et al (2004) Inhibition of mTOR induces autophagy and reduces toxicity of polyglutamine expansions in fly and mouse models of Huntington disease. Nat Genet 36:585–595
20. The Huntington's Disease Collaborative Group (1993) A novel gene containing a trinucleotide repeat that is expanded and unstable on Huntington's disease chromosomes. The Huntington's Disease Collaborative Research Group. Cell 72:971–983
21. Vonsattel JP, Myers RH, Stevens TJ, Ferrante RJ, Bird ED, Richardson EP Jr (1985) Neuropathological classification of Huntington's disease. J Neuropathol Exp Neurol 44:559–577
22. Labbadia J, Morimoto RI (2013) Huntington's disease: underlying molecular mechanisms and emerging concepts. Trends Biochem Sci 38:378–385
23. Zuccato C, Valenza M, Cattaneo E (2010) Molecular mechanisms and potential therapeutical targets in Huntington's disease. Physiol Rev 90:905–981
24. Vonsattel JP (2008) Huntington disease models and human neuropathology: similarities and differences. Acta Neuropathol 115:55–69
25. Francelle L, Galvan L, Brouillet E (2014) Possible involvement of self-defense mechanisms in the preferential vulnerability of the striatum in Huntington's disease. Front Cell Neurosci 8:295
26. Gines S, Ivanova E, Seong IS, Saura CA, MacDonald ME (2003) Enhanced Akt signaling is an early pro-survival response that reflects N-methyl-D-aspartate receptor activation in Huntington's disease knock-in striatal cells. J Biol Chem 278:50514–50522
27. Saavedra A, Garcia-Martinez JM, Xifro X, Giralt A, Torres-Peraza JF, Canals JM, Diaz-Hernandez M, Lucas JJ et al (2010) PH domain leucine-rich repeat protein phosphatase 1 contributes to maintain the activation of the PI3K/Akt pro-survival pathway in Huntington's disease striatum. Cell Death Differ 17:324–335
28. Giralt A, Saavedra A, Carreton O, Xifro X, Alberch J, Perez-Navarro E (2011) Increased PKA signaling disrupts recognition memory and spatial memory: role in Huntington's disease. Hum Mol Genet 20:4232–4247
29. Dragatsis I, Goldowitz D, Del MN, Deng YP, Meade CA, Liu L, Sun Z, Dietrich P et al (2009) CAG repeat lengths > or =335 attenuate the phenotype in the R6/2 Huntington's disease transgenic mouse. Neurobiol Dis 33:315–330
30. Mollersen L, Rowe AD, Larsen E, Rognes T, Klungland A (2010) Continuous and periodic expansion of CAG repeats in Huntington's disease R6/1 mice. PLoS Genet 6:e1001242
31. Morton AJ, Glynn D, Leavens W, Zheng Z, Faull RL, Skepper JN, Wight JM (2009) Paradoxical delay in the onset of disease caused by super-long CAG repeat expansions in R6/2 mice. Neurobiol Dis 33:331–341
32. Slow EJ, van RJ, Rogers D, Coleman SH, Graham RK, Deng Y, Oh R, Bissada N et al (2003) Selective striatal neuronal loss in a YAC128 mouse model of Huntington disease. Hum Mol Genet 12:1555–1567
33. Trettel F, Rigamonti D, Hilditch-Maguire P, Wheeler VC, Sharp AH, Persichetti F, Cattaneo E, MacDonald ME (2000) Dominant phenotypes produced by the HD mutation in STHdh(Q111) striatal cells. Hum Mol Genet 9:2799–2809
34. Rue L, Alcala-Vida R, Lopez-Soop G, Creus-Muncunill J, Alberch J, Perez-Navarro E (2014) Early down-regulation of PKCdelta as a pro-survival mechanism in Huntington's disease. NeuroMolecular Med 16:25–37
35. Puigdellivol M, Cherubini M, Brito V, Giralt A, Suelves N, Ballesteros J, Zamora-Moratalla A, Martin ED et al (2015) A role for Kalirin-7 in corticostriatal synaptic dysfunction in Huntington's disease. Hum Mol Genet 24:7265–7285
36. Anglada-Huguet M, Giralt A, Rue L, Alberch J, Xifro X (2016) Loss of striatal 90-kDa ribosomal S6 kinase (Rsk) is a key factor for motor, synaptic and transcription dysfunction in Huntington's disease. Biochim Biophys Acta 1862:1255–1266
37. Saavedra A, Giralt A, Rue L, Xifro X, Xu J, Ortega Z, Lucas JJ, Lombroso PJ et al (2011) Striatal-enriched protein tyrosine phosphatase expression and activity in Huntington's disease: a STEP in the resistance to excitotoxicity. J Neurosci 31:8150–8162
38. Rue L, Lopez-Soop G, Gelpi E, Martinez-Vicente M, Alberch J, Perez-Navarro E (2013) Brain region- and age-dependent dysregulation of p62 and NBR1 in a mouse model of Huntington's disease. Neurobiol Dis 52:219–228
39. Mangiarini L, Sathasivam K, Seller M, Cozens B, Harper A, Hetherington C, Lawton M, Trottier Y et al (1996) Exon 1 of the HD gene with an expanded CAG repeat is sufficient to cause a progressive neurological phenotype in transgenic mice. Cell 87: 493–506
40. Wheeler VC, Auerbach W, White JK, Srinidhi J, Auerbach A, Ryan A, Duyao MP, Vrbanac V et al (1999) Length-dependent gametic CAG repeat instability in the Huntington's disease knock-in mouse. Hum Mol Genet 8:115–122
41. Bashir T, Cloninger C, Artinian N, Anderson L, Bernath A, Holmes B, Benavides-Serrato A, Sabha N et al (2012) Conditional astroglial Rictor overexpression induces malignant glioma in mice. PLoS One 7:e47741
42. Chatterjee P, Seal S, Mukherjee S, Kundu R, Bhuyan M, Barua NC, Baruah PK, Babu SP et al (2015) A carbazole alkaloid deactivates mTOR through the suppression of rictor and that induces apoptosis in lung cancer cells. Mol Cell Biochem 405:149–158
43. Chen CC, Jeon SM, Bhaskar PT, Nogueira V, Sundararajan D, Tonic I, Park Y, Hay N (2010) FoxOs inhibit mTORC1 and activate Akt by inducing the expression of Sestrin3 and Rictor. Dev Cell 18: 592–604
44. Masri J, Bernath A, Martin J, Jo OD, Vartanian R, Funk A, Gera J (2007) mTORC2 activity is elevated in gliomas and promotes growth and cell motility via overexpression of rictor. Cancer Res 67:11712–11720
45. Masui K, Tanaka K, Akhavan D, Babic I, Gini B, Matsutani T, Iwanami A, Liu F et al (2013) mTOR complex 2 controls glycolytic

metabolism in glioblastoma through FoxO acetylation and upregulation of c-Myc. Cell Metab 18:726–739
46. Zhang C, Hwarng G, Cooper DE, Grevengoed TJ, Eaton JM, Natarajan V, Harris TE, Coleman RA (2015) Inhibited insulin signaling in mouse hepatocytes is associated with increased phosphatidic acid but not diacylglycerol. J Biol Chem 290:3519–3528
47. Holz MK, Blenis J (2005) Identification of S6 kinase 1 as a novel mammalian target of rapamycin (mTOR)-phosphorylating kinase. J Biol Chem 280:26089–26093
48. Nave BT, Ouwens M, Withers DJ, Alessi DR, Shepherd PR (1999) Mammalian target of rapamycin is a direct target for protein kinase B: identification of a convergence point for opposing effects of insulin and amino-acid deficiency on protein translation. Biochem J 344(Pt 2):427–431
49. Soliman GA, Acosta-Jaquez HA, Dunlop EA, Ekim B, Maj NE, Tee AR, Fingar DC (2010) mTOR Ser-2481 autophosphorylation monitors mTORC-specific catalytic activity and clarifies rapamycin mechanism of action. J Biol Chem 285:7866–7879
50. Kovacina KS, Park GY, Bae SS, Guzzetta AW, Schaefer E, Birnbaum MJ, Roth RA (2003) Identification of a proline-rich Akt substrate as a 14-3-3 binding partner. J Biol Chem 278: 10189–10194
51. Ortega Z, Diaz-Hernandez M, Maynard CJ, Hernandez F, Dantuma NP, Lucas JJ (2010) Acute polyglutamine expression in inducible mouse model unravels ubiquitin/proteasome system impairment and permanent recovery attributable to aggregate formation. J Neurosci 30:3675–3688
52. Gao D, Wan L, Inuzuka H, Berg AH, Tseng A, Zhai B, Shaik S, Bennett E et al (2010) Rictor forms a complex with Cullin-1 to promote SGK1 ubiquitination and destruction. Mol Cell 39:797–808
53. Uesugi A, Kozaki K, Tsuruta T, Furuta M, Morita K, Imoto I, Omura K, Inazawa J (2011) The tumor suppressive microRNA miR-218 targets the mTOR component Rictor and inhibits AKT phosphorylation in oral cancer. Cancer Res 71:5765–5778
54. Venkataraman S, Birks DK, Balakrishnan I, Alimova I, Harris PS, Patel PR, Handler MH, Dubuc A et al (2013) MicroRNA 218 acts as a tumor suppressor by targeting multiple cancer phenotype-associated genes in medulloblastoma. J Biol Chem 288:1918–1928
55. Bartel DP, Chen CZ (2004) Micromanagers of gene expression: the potentially widespread influence of metazoan microRNAs. Nat Rev Genet 5:396–400
56. Lee ST, Chu K, Im WS, Yoon HJ, Im JY, Park JE, Park KH, Jung KH et al (2011) Altered microRNA regulation in Huntington's disease models. Exp Neurol 227:172–179
57. Marti E, Pantano L, Banez-Coronel M, Llorens F, Minones-Moyano E, Porta S, Sumoy L, Ferrer I et al (2010) A myriad of miRNA variants in control and Huntington's disease brain regions detected by massively parallel sequencing. Nucleic Acids Res 38: 7219–7235
58. Packer AN, Xing Y, Harper SQ, Jones L, Davidson BL (2008) The bifunctional microRNA miR-9/miR-9* regulates REST and CoREST and is downregulated in Huntington's disease. J Neurosci 28:14341–14346
59. Diamanti D, Mori E, Incarnato D, Malusa F, Fondelli C, Magnoni L, Pollio G (2013) Whole gene expression profile in blood reveals multiple pathways deregulation in R6/2 mouse model. Biomark Res 1:28
60. Sancak Y, Thoreen CC, Peterson TR, Lindquist RA, Kang SA, Spooner E, Carr SA, Sabatini DM (2007) PRAS40 is an insulin-regulated inhibitor of the mTORC1 protein kinase. Mol Cell 25: 903–915
61. Vander HE, Lee SI, Bandhakavi S, Griffin TJ, Kim DH (2007) Insulin signalling to mTOR mediated by the Akt/PKB substrate PRAS40. Nat Cell Biol 9:316–323
62. Wang L, Harris TE, Roth RA, Lawrence JC Jr (2007) PRAS40 regulates mTORC1 kinase activity by functioning as a direct inhibitor of substrate binding. J Biol Chem 282:20036–20044
63. Carson RP, Fu C, Winzenburger P, Ess KC (2013) Deletion of Rictor in neural progenitor cells reveals contributions of mTORC2 signaling to tuberous sclerosis complex. Hum Mol Genet 22:140–152
64. Huang W, Zhu PJ, Zhang S, Zhou H, Stoica L, Galiano M, Krnjevic K, Roman G et al (2013) mTORC2 controls actin polymerization required for consolidation of long-term memory. Nat Neurosci 16: 441–448
65. Lebrun-Julien F, Bachmann L, Norrmen C, Trotzmuller M, Kofeler H, Ruegg MA, Hall MN, Suter U (2014) Balanced mTORC1 activity in oligodendrocytes is required for accurate CNS myelination. J Neurosci 34:8432–8448
66. Shiota C, Woo JT, Lindner J, Shelton KD, Magnuson MA (2006) Multiallelic disruption of the rictor gene in mice reveals that mTOR complex 2 is essential for fetal growth and viability. Dev Cell 11: 583–589
67. Wang S, Amato KR, Song W, Youngblood V, Lee K, Boothby M, Brantley-Sieders DM, Chen J (2015) Regulation of endothelial cell proliferation and vascular assembly through distinct mTORC2 signaling pathways. Mol Cell Biol 35:1299–1313
68. Chen X, Tagliaferro P, Kareva T, Yarygina O, Kholodilov N, Burke RE (2012) Neurotrophic effects of serum- and glucocorticoid-inducible kinase on adult murine mesencephalic dopamine neurons. J Neurosci 32:11299–11308
69. Wu X, Mao H, Liu J, Xu J, Cao J, Gu X, Cui G (2013) Dynamic change of SGK expression and its role in neuron apoptosis after traumatic brain injury. Int J Clin Exp Pathol 6:1282–1293
70. Gao D, Wan L, Wei W (2010) Phosphorylation of Rictor at Thr1135 impairs the Rictor/Cullin-1 complex to ubiquitinate SGK1. Protein Cell 1:881–885
71. Smrz D, Cruse G, Beaven MA, Kirshenbaum A, Metcalfe DD, Gilfillan AM (2014) Rictor negatively regulates high-affinity receptors for IgE-induced mast cell degranulation. J Immunol 193:5924–5932
72. Li J, Xu Z, Jiang L, Mao J, Zeng Z, Fang L, He W, Yuan W et al (2014) Rictor/mTORC2 protects against cisplatin-induced tubular cell death and acute kidney injury. Kidney Int 86:86–102
73. Garcia-Martinez JM, Perez-Navarro E, Xifro X, Canals JM, Diaz-Hernandez M, Trioulier Y, Brouillet E, Lucas JJ et al (2007) BH3-only proteins Bid and Bim(EL) are differentially involved in neuronal dysfunction in mouse models of Huntington's disease. J Neurosci Res 85:2756–2769
74. Urbanska M, Gozdz A, Swiech LJ, Jaworski J (2012) Mammalian target of rapamycin complex 1 (mTORC1) and 2 (mTORC2) control the dendritic arbor morphology of hippocampal neurons. J Biol Chem 287:30240–30256
75. Mazei-Robison MS, Koo JW, Friedman AK, Lansink CS, Robison AJ, Vinish M, Krishnan V, Kim S et al (2011) Role for mTOR signaling and neuronal activity in morphine-induced adaptations in ventral tegmental area dopamine neurons. Neuron 72:977–990